



# Stand age effects on Boreal forest physiology using a long time-series of satellite data



H. Croft<sup>a,\*</sup>, J.M. Chen<sup>a</sup>, T.L. Noland<sup>b</sup>

<sup>a</sup>University of Toronto, Department of Geography, Toronto, ON M5S 3G3, Canada

<sup>b</sup>Ontario Ministry of Natural Resources, Ontario Forest Research Institute, 1235 Queen St. E., Sault Ste. Marie, ON P6A 2E5, Canada

## ARTICLE INFO

### Article history:

Received 27 January 2014

Received in revised form 2 May 2014

Accepted 7 May 2014

Available online 16 June 2014

### Keywords:

Remote sensing

Reflectance

Leaf chlorophyll

LAI

Landsat

## ABSTRACT

Many ecosystem variables and processes show a relationship with stand age, including leaf area index (LAI), nutrient and water cycling, biomass production and photosynthesis. However, investigations into stand age dependency have typically focused on stand structure, and are limited by the availability of measurement sites. This study uses a measured chronosequence of 9 sites, ranging in age from 15 to 90 years, supported by a time-series of satellite-derived data to further validate temporal trends in LAI and leaf chlorophyll values. Managed *Pinus banksiana* stands in Northern Ontario, Canada were sampled for canopy structural parameters (LAI, stand density, crown radius, tree height) and leaf biochemistry (Chlorophyll a + b). Landsat 5 TM (30 m) data was obtained from 1989 to 2011 and chlorophyll- (Revised Transformed Chlorophyll absorption ratio index; RTCARI) and LAI- (Reduced Simple Ratio; RSR) sensitive spectral vegetation indices (VI) were calculated. Stand age showed strong relationships with tree height ( $R^2 = 0.95$ ,  $p < 0.001$ ), canopy radius ( $R^2 = 0.68$ ;  $p < 0.01$ ) and with stand density ( $R^2 = 0.49$ ;  $p < 0.01$ ). The measured LAI and leaf chlorophyll chronosequence showed an excellent correspondence with the VI-derived LAI and chlorophyll over time, modelled from the satellite archive. The temporal dependency of LAI and leaf chlorophyll with stand age was quantified through the fitting of a spherical model (chlorophyll = 44 years; LAI = 22 years), after which further increases in forest age did not increase leaf chlorophyll or LAI. Variation in the temporal lags indicates differences in the maturation period for leaf biochemistry and canopy physical structure, with LAI likely related to a reduction in stand density. The demonstrated stand age-dependency of leaf chlorophyll content is crucial for understanding stand age effects on photosynthetic processes and carbon assimilation, both for quantifying net primary production (NPP) within carbon budgets and for guiding forest management and harvesting strategies in light of a changing climate.

© 2014 Elsevier B.V. All rights reserved.

## 1. Introduction

Forest age affects ecological attributes such as biodiversity, leaf area index (LAI), biomass production, NPP, and nutrient and water cycling, with aboveground NPP being found to reach a peak early in stand development and then gradually decline by mean reduction of 34% (Gower et al., 1996). Rapid tree growth in early development means that young forests have the potential to sequester a large amount of carbon (Houghton et al., 2009), relative to old growth forests, although individual tree carbon sequestration rates can increase with age (Stephenson et al., 2014). The dependency of ecological processes on tree age is particularly important in areas which are subject to frequent disturbance, for example through

fire, insects, extreme weather, land use change and harvesting (Schroeder et al., 2011; Wulder et al., 2010). Clearcut harvesting results in the removal of biomass, the loss of important habitat structures, such as coarse woody debris, and a decline in insect and animal communities (Niemelä, 1999). Monitoring the rate and successive development of forest re-establishment following harvest is therefore important for a number of ecological processes, including nutrient cycling, carbon storage potential and habitat structures (Schroeder et al., 2007). As forest disturbance often affects large land areas, it has been identified as a key driver of forest net carbon balance (Gough et al., 2007; Kurz et al., 2009; Schroeder et al., 2011). Although there has been considerable research into changes in forest structural composition (i.e. LAI, biomass, stand density), there has been little interest in leaf biochemistry, such as chlorophyll content. Leaf chlorophyll plays a central role in the conversion of solar radiation via photosynthesis into

\* Corresponding author. Tel.: +1 4169783375.

E-mail address: [holly.croft@utoronto.ca](mailto:holly.croft@utoronto.ca) (H. Croft).

stored chemical energy (Gitelson et al., 2006). As chlorophyll concentration largely determines the amount of photosynthetically active solar radiation absorbed by the leaf, low concentrations of chlorophyll can limit photosynthetic potential and hence primary productivity (Ellsworth and Reich, 1993; Koike et al., 2004; Richardson et al., 2002). Forest NPP is closely related to forest age, with NPP increasing rapidly during early development stages, reaching a maximum towards middle age and gradually declining in later stages (Chen et al., 2002b; He et al., 2012; Wang et al., 2011). Franklin et al. (2002) define the first 20 years following disturbance as cohort establishment followed by canopy closure, with biomass accumulation occurring from around 30–90 years of age, depending on the species. A maturation stage begins as biomass accumulation levels off by reaching an asymptote around 70–100 years in Douglas-fir (Franklin et al., 2002).

Substituting space-for-time is widely used in ecological modeling to infer past or future trajectories from measured spatial patterns (Blois et al., 2013), based on assumptions that sites are not affected by underlying spatial controls and instead represent temporal dynamics of the parameter of interest. Here we use a space-for-time substitution approach to develop a chronosequence to investigate variations in stand structure and leaf chlorophyll content over a long-term time frame. To support the information derived from multiple spatial sites, satellite data was used to re-sample each site at regular time intervals to assess the changes at a per site level (Foster and Tilman, 2000). The longevity of Landsat missions offers an unparalleled resource of high quality satellite images, at fine spatial resolution (30 m) and regular revisit intervals (circa 16 days). Previous studies have used Landsat time series to derive a wide range of forest applications, including resource management (Wilson and Sader, 2002) and pest mortality (Goodwin et al., 2010). Schroeder et al. (2007) used a multi-temporal image series to create “re-growth trajectories” comprised of a series of mathematical or statistical models used to characterize vegetation response to disturbance. In this study we examined nine Jack Pine (*Pinus banksiana* Lamb.) stands of varying ages (from 15 to 90 years old) within a managed forestry environment to assess the effect that stand age has on physical and biochemical parameters, at the canopy and leaf level. The objectives of this work are to: (1) examine the differences in stand structure across a range of stand ages; (2) investigate if LAI and leaf chlorophyll content varies with stand age; (3) develop a chronosequence from satellite time-series data to monitor changes at a site level.

## 2. Methods

### 2.1. Study sites

Nine jack pine (*P. banksiana* Lamb.) (JP) stands located southeast of Chapleau, Ontario (47°36'17"N to 47°33'40"N, and 83°08'23"W to 82°43'04"W) were sampled. Stand ages ranged from approximately 15- to 90-years-old (Fig. 1) and all stands were greater than

100 ha in area. The sites are underlain by well-drained silt loam soils over deep gravelly sand, with mean annual temperatures of 4.6 °C and annual precipitation of 871 mm (Zhu et al., 2004). Understorey species included dense moss, upland willow (*Salix humilis*), blueberries (*Vaccinium* spp.) and grasses.

### 2.2. Ground measurements

Leaf chlorophyll content ( $\mu\text{g}/\text{cm}^2$ ) and a range of structural parameters were measured at each field sampling site from the 16th–19th July, 2012. Leaves and shoots were sampled from the upper sunlit canopy using a shotgun, sealed in plastic bags and kept at a temperature below 0 °C for further analysis (Zhang et al., 2007). This process was performed on five representative trees within each stand, approximately 50–100 m apart and three branches from each sampled tree canopy, giving 15 samples per stand. Mature needles (i.e. not current year) were systematically sampled from the top of canopy branches, with one needle leaf taken from each year's growth and homogenised into one sample for laboratory leaf chlorophyll analysis. Foliar chlorophyll was extracted using spectranalysed grade *N,N*-dimethylformamide, and absorbance measured at 663.8 nm, 646.8 nm, and 480 nm using a Cary-1 spectrophotometer (Wellburn, 1994). The measured leaf chlorophyll values reported in this study were calculated as mean values from all leaf samples collected within each site. Total leaf chlorophyll (Chl a + b) content ( $\mu\text{g}/\text{cm}^2$ ) was measured using the method reported by (Moorthy et al., 2008). Effective LAI ( $L_e$ ) was measured using the LAI-2000 plant canopy analyzer (Li-Cor, Lincoln, NE, USA) (Chen et al., 1997). The element clumping index and leaf area index were measured using TRAC (Tracing Radiation and Architecture of Canopies) (Chen and Cihlar, 1995). Both the LAI2000 and TRAC measurements were collected across a 100 m transect at 10 m intervals within each stand. Additional stand structural parameters including tree height, canopy radius and tree density were also measured (Table 1).

### 2.3. Landsat 5 TM data acquisition and processing

Ten Landsat 5 TM scenes were acquired from 1989 through to 2011 (Landsat TM 5 suffered a mechanical failure in 2012) at 30 m spatial resolution. The scenes were selected to match as closely as possible the time frame of ground data collection (16–19th July, 2012), and are representative of the middle of the growing season (Table 2). The coarse temporal resolution of Landsat acquisition (every 16 days) and cloudy skies makes exact correspondence very difficult to achieve. As a consequence there are gaps in the annual sequence due to a lack of availability of cloud-free images.

Landsat 5 TM images were radiometrically and geometrically corrected and georeferenced to UTM map projection. The geometric accuracy of the images is usually between 30 and 50 m. The Landsat scenes were atmospherically corrected using cosine estimation of atmospheric transmittance (Chavez Jr., 1996). Whilst radiative



Fig. 1. Locations of the Jack Pine stands of varying ages. Source: Google earth.

**Table 1**  
Site characteristics and ground measurement data.

Stand ID	Year established	Age (years) <sup>a</sup>	Height (m)	Crown radius (m)	Density (trees/ha)	LAI	Clumping index
JP04	1975	37	14	1.78	800	3.59	0.86
JP07	1952	60	17	1.81	1400	3.19	0.93
JP10	1994	18	4	1.37	2370	1.37	0.88
JP12	1957	55	16	2.50	1870	2.84	0.86
JP14	1993	19	8	1.79	1500	2.66	0.89
JP15	1997	15	7	1.55	4730	4.13	0.89
JP22	1991	21	7	1.61	1930	2.59	0.94
JP23	1993	19	6	1.72	3030	4.32	0.90
JP41	1922	90	24	2.50	970	2.82	0.83

<sup>a</sup> Age is relative to ground measurement date in 2012.

**Table 2**  
Landsat 5 TM image acquisition information.

Date	19/08/1989	22/08/1990	25/08/1997	12/08/1998	04/08/2001	09/08/2002	21/08/2007	06/07/2008	29/08/2010	16/08/2011
Path	21, 27	21, 27	21, 27	21, 27	21, 27	21, 27	21, 27	21, 27	21, 27	21, 27
SZA/VZA (°)	42, 0	43, 0	43, 0	38, 0	36, 0	47, 0	39, 0	31, 0	42, 0	38, 0

transfer methods (e.g. 6S and MODTRAN (Berk et al., 1998; Vermote et al., 1997)) can produce more accurate results, they usually require coincident atmospheric measurements such as aerosol optical depth, water vapour and ozone, to parameterise the model (Sharma et al., 2009). Mahiny and Turner (2007) found that 6S produced anomalous results when all the detailed data on atmospheric condition that is required was not used. As these measurements were not available, this study used the COST method (Chavez Jr., 1996), which is an absolute image-based method (Mahiny and Turner, 2007), where the cosine of sun zenith angle is used to approximate the effects of absorption by atmospheric gases and Rayleigh scattering for individual spectral bands (Eq. (1)),

$$\rho = \pi * d^2 * (L_{\lambda\text{sat}} - L_{\lambda\text{haze}}) / \text{ESUN}_{\lambda} * \cos^2 \theta \quad (1)$$

where  $p$  = reflectance factor;  $L_{\lambda\text{sat}}$  = spectral radiance at the sensor;  $L_{\lambda\text{haze}}$  = path radiance;  $d$  = earth–sun distance (AU); ESUN = mean solar exoatmospheric irradiances;  $\theta$  = solar zenith angle (°). The solar exoatmospheric spectral irradiances (ESUN) for the Landsat 5 TM were obtained from Chander and Markham (2003). Path radiance ( $L_{\lambda\text{haze}}$ ) was obtained from pixels of known zero reflectance such as large deep water bodies and it was assumed that any value in the raw image in these areas other than zero represented haze effects. This value was subsequently verified through a band specific histogram analysis by examining the step in pixel radiance values, usually occurring at 1% for the image (Chavez Jr., 1988).

#### 2.4. Spectral vegetation indices

This study uses empirical vegetation indices to derive leaf chlorophyll content and LAI from satellite-derived reflectance data. Within the visible part of the electromagnetic spectrum, chlorophyll is known to have strong absorption features in blue (~490 nm) and red (~680 nm) wavelengths, and maximum reflectance in green wavelengths (~560 nm). Conversely, the NIR wavelengths are dominated by structural effects and canopy architecture. The Transformed Chlorophyll absorption ratio index (TCARI) was adapted from the Modified Chlorophyll Absorption Ratio Index due to a sensitivity to non-photosynthetic elements effects, and revised (RTCARI) further by Wu et al. (2008) to increase the linearity of its relationship with chlorophyll content (Eq. (2)). In a recent study, Croft et al. (2014) found that RTCARI was the best performing vegetation index (out of 47 tested) for coniferous trees at the canopy level. RTCARI is calculated as follows:

$$\text{RTCARI} = 3 * [(R_{750} - R_{705}) - 0.2 * (R_{750} - R_{550})] * \left( \frac{R_{750}}{R_{705}} \right) \quad (2)$$

The reduced bandset of Landsat images meant that for this study, the NIR band at 750 nm was replaced by the Landsat band centred at 830 nm, and the 705 nm wavelength at the base of the red-edge was replaced by the red band centred at 660 nm.

To model LAI variations over time and space, the Reduced Simple Ratio (RSR) was selected, due to its improved linearity with LAI, in comparison to other structural indices such as NDVI, therefore reducing the effects of saturation at high LAI values (Chen et al., 2002a). The RSR is calculated as follows (Eq. (3)):

$$\text{RSR} = \frac{\rho_{\text{NIR}}}{\rho_{\text{red}}} \left( 1 - \frac{\rho_{\text{SWIR}} - \rho_{\text{SWIR min}}}{\rho_{\text{SWIR max}} - \rho_{\text{SWIR min}}} \right) \quad (3)$$

where  $\rho_{\text{NIR}}$ ,  $\rho_{\text{red}}$ , and  $\rho_{\text{SWIR}}$  are the reflectance in NIR, red, and SWIR band, respectively. Minimum and maximum SWIR reflectance ( $\rho_{\text{SWIR min}}$  and  $\rho_{\text{SWIR max}}$ ) were defined as the 1% minimum and maximum cut-off in SWIR reflectance histograms for each Landsat scene. Further advantages of RSR are a reduced sensitivity to different land cover types and reduction in background/understorey influences because the SWIR band is most sensitive to the amount of vegetation containing liquid water in the background. The latter is particularly important in areas of low canopy coverage. LAI values were subsequently modelled using empirical algorithm developed by Chen et al. (2002a, b) in a comprehensive study of different land covers across Canada.

$$\text{LAI} = \text{RSR} / 1.242 \quad (4)$$

The relationship between measured leaf chlorophyll content and RTCARI, and measured and modelled LAI are shown in Fig. 2a and b.

Fig. 2 demonstrates a very strong relationship between leaf chlorophyll and RTCARI, confirming results found for other coniferous species (Croft et al., 2014). The modelled LAI (from RSR; Chen et al., 2002a,b) and measured LAI also shows a good relationship, although a slight overestimation of LAI values at JP10 reduces the coefficient of determination.

#### 2.5. Quantifying temporal thresholds in stand age physiological relationships

Spherical models are often used in geostatistics to statistically describe the spatial scale of variation in a dataset (Croft et al., 2013a), where an asymptote denotes the maximum extent of spatially correlated variance. Here the spherical model (Eq. (5)) is fitted to the satellite time-series data in order to quantify the age at which an asymptote is reached ( $\alpha$  = range distance), therefore

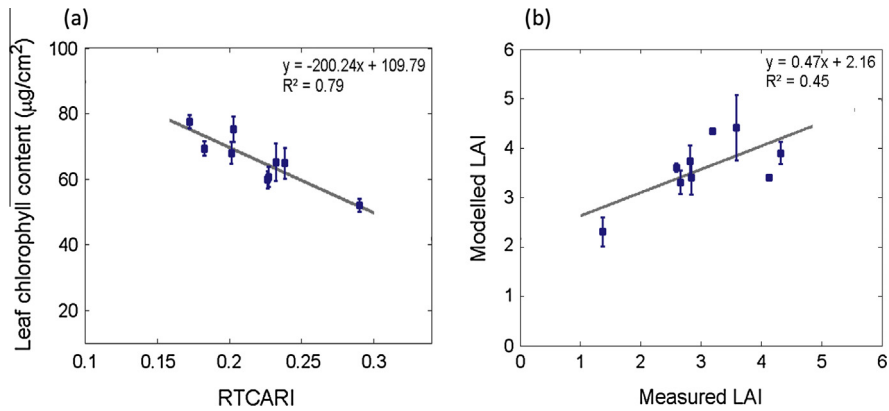


**Fig. 2.** Relationships between (a) measured chlorophyll content and RTCARI ( $p < 0.005$ , RMSE = 0.015 µg/cm<sup>2</sup>), and (b) measured LAI and modelled LAI from an empirical RSR algorithm ( $p < 0.05$ ; RMSE = 0.96 m<sup>2</sup>/m<sup>2</sup>). Error bars represent the standard error.

signifying that further increases in stand age do not result in subsequent changes in leaf chlorophyll or LAI. Eq. (5) gives details of the spherical model fitted to the time-series; where  $y_{mod}$  is the modelled parameter (LAI or chlorophyll) for a given time lag ( $h$ ),  $c_T$  is the maximum  $y$  parameter value and ( $c_0$ ) the sum of  $y$  intercept, with  $c_1$  the being difference, if  $h \leq a$ .  $c_T = c_0 + c_1$  where  $y_{mod}(h) = c_T$  if  $h > a$  (Deutsch and Journel, 1998).

$$y_{mod}(h) = c_1 \left[ 1.5 \frac{h}{a} - 0.5 \left( \frac{h}{a} \right)^3 \right] + c_0 \quad (5)$$

### 3. Results and discussion

#### 3.1. Measured tree growth patterns across a chronosequence

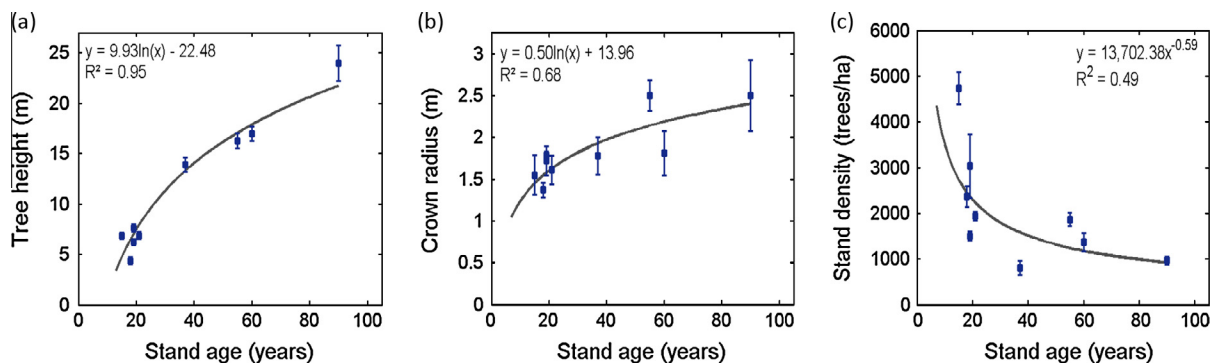
Changes in tree and stand structure with increasing tree age have been noted by several authors (Long and Smith, 1992; Peichl and Arain, 2006; Schlerf et al., 2005), however the nature of these changes can depend on the specific ecological parameter measured, with not all tree variables changing linearly or in temporal uniformity with increasing age. The changes in tree height, crown radius and stand density across the measured chronosequence (15–90 years old) are shown in Fig. 3.

Fig. 3 shows a strong curvilinear log relationship ( $R^2 = 0.95$ ) between tree height and stand age, whilst stand density appears to decrease rapidly up to approximately 40 years of age and then subsequently levels off. This result supports the conceptual model suggested by Franklin et al. (2002), where after the biomass accumulation growth stage reaches an asymptote, trees continue to

increase in height, but stand density remains fairly stable. The crown radius measurements indicate a weaker linear relationship with stand age ( $R^2 = 0.68$ ), which could be due a result of a lack of availability of older sites in the dataset reaching the maturation stage, which sees the trees attain maximum crown spread (Franklin et al., 2002).

#### 3.2. Temporal changes in leaf chlorophyll content and LAI at each site from a Landsat time-series

Deriving leaf chlorophyll and LAI data from satellite-derived reflectance data has received considerable research focus, due to their key roles in plant photosynthesis and energy and water fluxes, and methods are well-developed (Chen et al., 2002a, 1997; Croft et al., 2013b; Zhang et al., 2008). Consequently, a long time series of Landsat data can be used to allow a temporal re-sampling at each site in the chronosequence to better validate any time-dependent dynamics in these variables (Foster and Tilman, 2000). The modelled changes in leaf chlorophyll and LAI from satellite data show increasing values for both parameters in the earlier stages of re-growth, followed by a levelling off period (Fig. 4). However, the leaf chlorophyll values increase more gradually with stand age, and begin to plateau at a later age (~40–50 years). In comparison, the LAI values reveal a sharp increase until an asymptote is reached at ~20 years, after which the values do not increase. This result is supported by the ground measurements of structural parameters in Fig. 3, which show a levelling off of canopy radius and stand density values after approximately 20 years. Crown closure of well-stocked JP stands usually occurs by about 20 years, which is likely is the main driver for the LAI



**Fig. 3.** Measured tree structural properties for all sites, where (a) tree height ( $p < 0.001$ , RMSE = 1.37 m); (b) crown radius ( $p < 0.01$ , RMSE = 0.21 m); (c) stand density ( $p < 0.01$ ; RMSE = 832 trees/ha). Error bars represent the standard error.

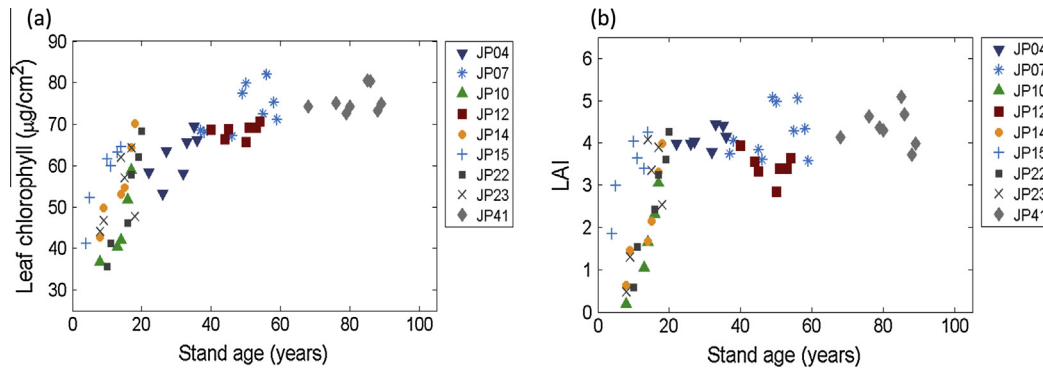


Fig. 4. Satellite-derived estimates of (a) leaf chlorophyll content; and (b) LAI across a chronosequence from 1989 to 2011 using Landsat 5 TM data.

peak value (Vose et al., 1994). Crown closure in jack pine has been shown to be the dominant factor influencing the spectral response in Landsat TM images (Franklin et al., 2002). Whilst the results in Fig. 4 show strong trends with age, there is some scatter in the modelled values within each site by year, which could be due to error as a result of atmospheric scattering or BRDF effects, or due to changes at site level. Chlorophyll content is known to vary according to plant stress (Carter and Knapp, 2001), for example and LAI variations may occur due to thinning and other management actions, or from extreme weather events.

### 3.3. Quantifying temporal differences in chlorophyll content and LAI

In order to quantify the temporal relationship between leaf chlorophyll and LAI, spherical models were fitted to the data to extract the stand age where an asymptote is reached for each variable (Fig. 5). Additionally, the measured leaf chlorophyll values from ground sampling in 2012 are shown for comparison alongside the modelled chlorophyll estimates from the Landsat time-series.

The measured chlorophyll values show a good fit within the modelled chlorophyll chronosequence, indicating that the use of the Landsat archive has produced reliable results. The additional data points derived from modelled Landsat data supports the trend shown by the measured data. The LAI measured data broadly support the modelled LAI values, particularly in the early- and mid- stand ages. There is some discrepancy in the older stands, particularly JP41 (90 years old), where the measured data are lower than the modelled satellite estimates. This could have been due to measurement error in ground sampling or overestimations arising due to incomplete crown cover and a well-developed understory, including smaller trees. The fitted spherical models

quantitatively demonstrate the temporal differences in the development of stand physical and biochemical variables. Leaf chlorophyll has a range value of 44 years, compared to LAI which is 22 years. The levelling off of LAI values may be due to crown closure and the reduction in stand density, shown in Fig. 3c, which also occurs around 20 years. The stabilisation of chlorophyll values at mid growth stages (44 years) does not appear to be related to forest structural changes, and may be related to nitrogen availability, which has been found to decline with age as it becomes immobilized in woody biomass (Murty and McMurtrie, 2000). However, other studies have found no evidence of decreases in nitrogen availability, and this may be ecosystem or site specific, depending on nitrogen uptake from soil nitrogen pools (Drake et al., 2010; Johnson, 2006; Smithwick et al., 2009).

### 3.4. Changes in leaf chlorophyll and LAI values from 1989 to 2010

The positive and negative changes in leaf chlorophyll and LAI between 2010 and 2001 are mapped in Fig. 6. The images of 1989 and 2010 were used because they represent earliest date after all plantations within this study have been established (1997; PJ15) and latest date with all sites cloud-free. The largest changes in both LAI and chlorophyll are for managed stands, that have either been harvested since 2001 (large negative change) or have undergone re-growth since 2001 (large positive change). For chlorophyll this typically represents changes of around 20–30  $\mu\text{g}/\text{cm}^2$ , which corresponds to the results in Fig. 4. Any extreme values of chlorophyll and LAI outside the measured range of values contain a degree of uncertainty, as empirical relationships between the vegetation index and stand property are only inferred through the regression line, and not mathematically demonstrated.

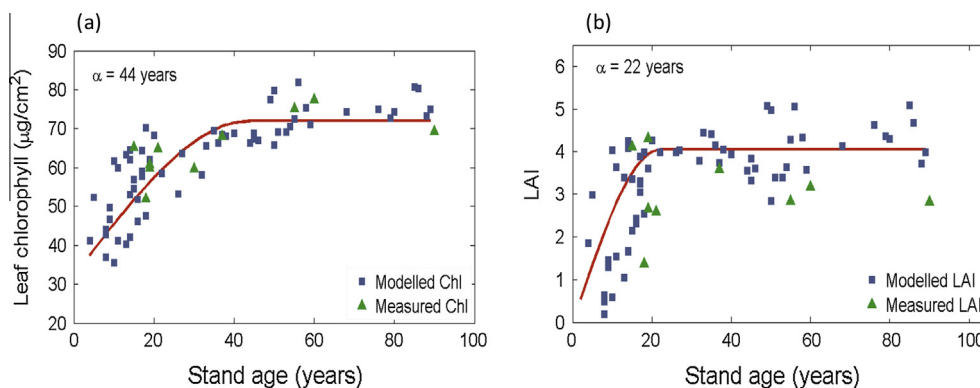


Fig. 5. Spherical model fitted to modelled chlorophyll content from Landsat-derived data from 1989 to 2010, alongside measured ground data, for (a) Chlorophyll content and (b) LAI, where  $\alpha$  = range value.

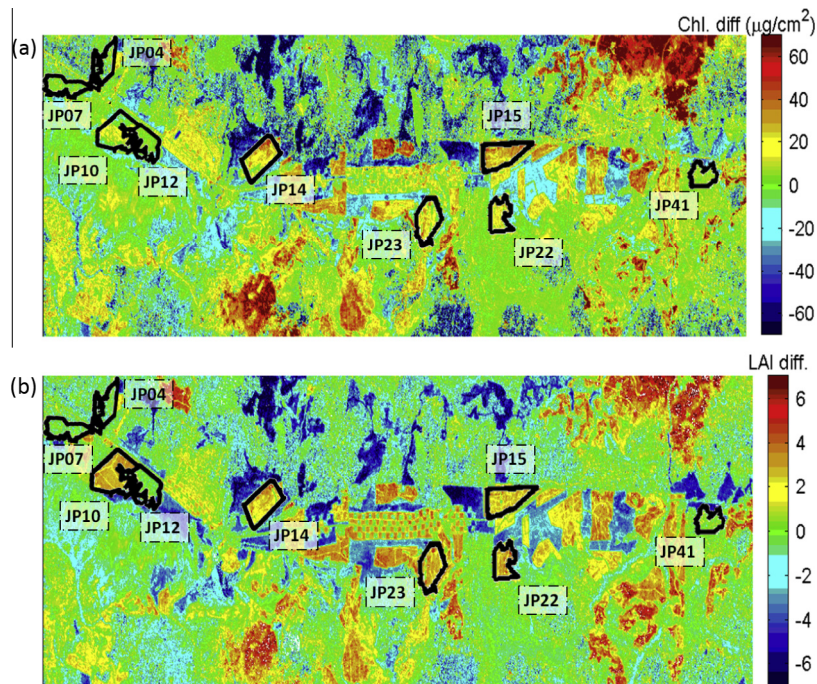


Fig. 6. Mapped changes in (a) leaf chlorophyll and (b) LAI values from 2001 to 2010.

Over the sampled time period, increases in LAI at re-growth sites are typically around LAI = 2–3, whereas for any harvested stands, the drop is around LAI = 4. In the managed stands, the spatial and temporal variations in leaf chlorophyll content and LAI values typically agree. In the less obviously managed areas of forest, leaf chlorophyll appears to stay neutral or slightly increase across large areas of land. LAI also remained relatively consistent, with slightly larger areas showing small declines in LAI. These differences may be attributable to the point in the forest's growth stage, which is demonstrated in Fig. 5; where changes in LAI and leaf chlorophyll appear to occur at different rates and over different temporal ranges.

These findings have potentially far reaching implications for the monitoring of carbon assimilation and biomass accumulation in the managed *P. banksiana* plantations. As chlorophyll is the 'photosynthetic apparatus' of the plant (Peng et al., 2013), only the PAR absorbed by chlorophyll is used for photosynthesis (Zhang et al., 2009). As a result, studies have demonstrated that leaf chlorophyll content is well correlated with temporal changes in light use efficiency (Peng et al., 2011; Wu et al., 2009) and between canopy chlorophyll content and GPP (Gitelson et al., 2003, 2006; Peng et al., 2011). The stabilisation of chlorophyll content at a stand age of 44 years correlates with the temporal dependency of NPP to stand age, where NPP increases rapidly at the early development stage, reaches a maximum in middle ages and gradually declines in later ages. He et al. (2012) found that the stand-age-NPP curve peaked at approximately 35 years for Jack Pine. These results may inform management decisions for optimising harvest ages, in order to maximise productivity increases within a given time-scale and reduce atmospheric CO<sub>2</sub> levels by managing the age-class structure of forested landscapes (He et al., 2012).

#### 4. Conclusion

Our research has shown that, along with the well-known changes in stand structure with tree age, leaf biochemistry also shows a high level of age dependency. The difference in chlorophyll

content between young and old needles is well known, but these findings indicate that for mature needles, tree age also affects stand chlorophyll concentration. This has important implications for better understanding and mapping the changes in photosynthetic processes and NPP. Leaf chlorophyll content showed a strong temporal correlation with stand age, which was quantified through the fitting of a spherical model. This temporal dependence for chlorophyll was 44 years, after which no further increase in forest age resulted in an increase in leaf chlorophyll. Conversely, the temporal lag for LAI was much shorter, at 22 year old, demonstrating differences in the maturation period for leaf biochemistry and canopy physical structure. These results represent the first important stages of investigating age dependency in needle leaf chlorophyll content. Further work is needed to better understand how leaf chlorophyll responds to nitrogen availability, and other factors thought to limit NPP, such as stomatal conductance and hydraulic limitation.

#### References

- Berk, A., Bernstein, L., Anderson, G., Acharya, P., Robertson, D., Chetwynd, J., Adler-Golden, S., 1998. MODTRAN cloud and multiple scattering upgrades with application to AVIRIS. *Remote Sens. Environ.* 65, 367–375.
- Blois, J.L., Williams, J.W., Fitzpatrick, M.C., Jackson, S.T., Ferrier, S., 2013. Space can substitute for time in predicting climate-change effects on biodiversity. *Proceedings of the National Academy of Sciences*.
- Carter, G.A., Knapp, A.K., 2001. Leaf optical properties in higher plants: linking spectral characteristics to stress and chlorophyll concentration. *Am. J. Bot.* 88, 677–684.
- Chander, G., Markham, B., 2003. Revised Landsat-5 TM radiometric calibration procedures and postcalibration dynamic ranges. *Geosci. Remote Sens., IEEE Trans.* 41, 2674–2677.
- Chavez Jr., P.S., 1988. An improved dark-object subtraction technique for atmospheric scattering correction of multispectral data. *Remote Sens. Environ.* 24, 459–479.
- Chavez Jr., P.S., 1996. Image-based atmospheric corrections-revisited and improved. *Photogramm. Eng. Remote Sens.* 62, 1025–1036.
- Chen, J.M., Cihlar, J., 1995. Quantifying the effect of canopy architecture on optical measurements of leaf area index using two gap size analysis methods. *Geosci. Remote Sens., IEEE Trans.* 33, 777–787.
- Chen, J.M., Plummer, P.S., Rich, M., Gower, S.T., Norman, J.M., 1997. Leaf area index measurements. *J. Geophys. Res.* 102, 29–429.

- Chen, J.M., Pavlic, G., Brown, L., Cihlar, J., Leblanc, S.G., White, H.P., Hall, R.J., Peddle, D.R., King, D.J., Trofymow, J.A., 2002a. Derivation and validation of Canada-wide coarse-resolution leaf area index maps using high-resolution satellite imagery and ground measurements. *Remote Sens. Environ.* 80, 165–184.
- Chen, W., Chen, J.M., Price, D.T., Cihlar, J., 2002b. Effects of stand age on net primary productivity of Boreal black spruce forests in Ontario, Canada. *Can. J. For. Res.* 32, 833–842.
- Croft, H., Anderson, K., Brazier, R.E., Kuhn, N.J., 2013a. Modeling fine-scale soil surface structure using geostatistics. *Water Resour. Res.* 49, 1858–1870.
- Croft, H., Chen, J.M., Zhang, Y., Simic, A., 2013b. Modelling leaf chlorophyll content in broadleaf and needle leaf canopies from ground, CASI, Landsat TM 5 and MERIS reflectance data. *Remote Sens. Environ.* 133, 128–140.
- Croft, H., Chen, J.M., Zhang, Y., 2014. The applicability of empirical vegetation indices for determining leaf chlorophyll content over different leaf and canopy structures. *Ecol. Complex.* 17, 119–130.
- Deutsch, C., Journel, A., 1998. *GSLIB: Geostatistical software library and users guide*, second ed. Oxford University Press, New York.
- Drake, J.E., Raetz, L.M., Davis, S.C., DeLucia, E.H., 2010. Hydraulic limitation not declining nitrogen availability causes the age-related photosynthetic decline in loblolly pine (*Pinus taeda* L.). *Plant, Cell Environ.* 33, 1756–1766.
- Ellsworth, D., Reich, P., 1993. Canopy structure and vertical patterns of photosynthesis and related leaf traits in a deciduous forest. *Oecologia* 96, 169–178.
- Foster, B., Tilman, D., 2000. Dynamic and static views of succession: testing the descriptive power of the chronosequence approach. *Plant Ecol.* 146, 1–10.
- Franklin, J.F., Spies, T.A., Pelt, R.V., Carey, A.B., Thornburgh, D.A., Berg, D.R., Lindenmayer, D.B., Harmon, M.E., Keeton, W.S., Shaw, D.C., Bible, K., Chen, J., 2002. Disturbances and structural development of natural forest ecosystems with silvicultural implications, using Douglas-fir forests as an example. *For. Ecol. Manage.* 155, 399–423.
- Gitelson, A.A., Verma, S.B., Vina, A., Rundquist, D.C., Keydan, G., Leavitt, B., Arkebauer, T.J., Burba, G.G., Suyker, A.E., 2003. Novel technique for remote estimation of CO<sub>2</sub> flux in maize. *Geophys. Res. Lett.* 30, 31–39.
- Gitelson, A.A., Viña, A., Verma, S.B., Rundquist, D.C., Arkebauer, T.J., Keydan, G., Leavitt, B., Ciganda, V., Burba, G.G., Suyker, A.E., 2006. Relationship between gross primary production and chlorophyll content in crops: implications for the synoptic monitoring of vegetation productivity. *J. Geophys. Res. D: Atmos.* 111.
- Goodwin, N.R., Magnussen, S., Coops, N.C., Wulder, M.A., 2010. Curve fitting of time-series Landsat imagery for characterizing a mountain pine beetle infestation. *Int. J. Remote Sens.* 31, 3263–3271.
- Gough, C.M., Vogel, C.S., Harrold, K.H., George, K., Curtis, P.S., 2007. The legacy of harvest and fire on ecosystem carbon storage in a north temperate forest. *Glob. Change Biol.* 13, 1935–1949.
- Gower, S.T., McMurtrie, R.E., Murty, D., 1996. Aboveground net primary production decline with stand age: potential causes. *Trends Ecol. Evol.* 11, 378–382.
- He, L., Chen, J.M., Pan, Y., Birdsey, R., Katge, J., 2012. Relationships between net primary productivity and forest stand age in U.S. forests. *Global Biogeochemical Cycles* 26, GB3009.
- Houghton, R.A., Hall, F., Goetz, S.J., 2009. Importance of biomass in the global carbon cycle. *J. Geophys. Res. Biogeosci.* 114, G00E03.
- Johnson, D.W., 2006. Progressive N limitation in forests: review and implications for long-term responses to elevated CO<sub>2</sub>. *Ecology* 87, 64–75.
- Koike, T., Kitaoka, S., Ichie, T., Lei, T., Kitao, M., 2004. Photosynthetic Characteristics of Mixed Deciduous-Broadleaf Forests from Leaf to Stand. *Global environmental change in the ocean and on land*, Tokyo, Terrapub, pp. 453–472.
- Kurz, W.A., Dymond, C.C., White, T.M., Stinson, G., Shaw, C.H., Rampley, G.J., Smyth, C., Simpson, B.N., Neilson, E.T., Trofymow, J.A., Metsaranta, J., Apps, M.J., 2009. CBM-CFS3: A model of carbon-dynamics in forestry and land-use change implementing IPCC standards. *Ecol. Model.* 220, 480–504.
- Long, J.N., Smith, F.W., 1992. Volume increment in *Pinus contorta* var. *latifolia*: the influence of stand development and crown dynamics. *For. Ecol. Manage.* 53, 53–64.
- Mahiny, A.S., Turner, B.J., 2007. A comparison of four common atmospheric correction methods. *Photogramm. Eng. Remote Sens.* 73, 361.
- Moorthy, I., Miller, J.R., Noland, T.L., 2008. Estimating chlorophyll concentration in conifer needles with hyperspectral data: an assessment at the needle and canopy level. *Remote Sens. Environ.* 112, 2824–2838.
- Murty, D., McMurtrie, R.E., 2000. The decline of forest productivity as stands age: a model-based method for analysing causes for the decline. *Ecol. Model.* 134, 185–205.
- Niemelä, J., 1999. Management in relation to disturbance in the Boreal forest. *For. Ecol. Manage.* 115, 127–134.
- Peichl, M., Arain, M.A., 2006. Above- and belowground ecosystem biomass and carbon pools in an age-sequence of temperate pine plantation forests. *Agric. For. Meteorol.* 140, 51–63.
- Peng, Y., Gitelson, A.A., Keydan, G., Rundquist, D.C., Moses, W., 2011. Remote estimation of gross primary production in maize and support for a new paradigm based on total crop chlorophyll content. *Remote Sens. Environ.* 115, 978–989.
- Peng, Y., Gitelson, A.A., Sakamoto, T., 2013. Remote estimation of gross primary productivity in crops using MODIS 250m data. *Remote Sens. Environ.* 128, 186–196.
- Richardson, A.D., Duigan, S.P., Berlyn, G.P., 2002. An evaluation of noninvasive methods to estimate foliar chlorophyll content. *New Phytol.* 153, 185–194.
- Schlerf, M., Atzberger, C., Hill, J., 2005. Remote sensing of forest biophysical variables using HyMap imaging spectrometer data. *Remote Sens. Environ.* 95, 177–194.
- Schroeder, T.A., Cohen, W.B., Yang, Z., 2007. Patterns of forest regrowth following clearcutting in western Oregon as determined from a Landsat time-series. *For. Ecol. Manage.* 243, 259–273.
- Schroeder, T.A., Wulder, M.A., Healey, S.P., Moisen, G.G., 2011. Mapping wildfire and clearcut harvest disturbances in Boreal forests with Landsat time series data. *Remote Sens. Environ.* 115, 1421–1433.
- Sharma, A.R., Badarinath, K., Roy, P., 2009. Comparison of ground reflectance measurement with satellite derived atmospherically corrected reflectance: a case study over semi-arid landscape. *Adv. Space Res.* 43, 56–64.
- Smithwick, E.H., Kashian, D., Ryan, M., Turner, M., 2009. Long-term nitrogen storage and soil nitrogen availability in post-fire lodgepole pine ecosystems. *Ecosystems* 12, 792–806.
- Stephenson, N.L., Das, A.J., Condit, R., Russo, S.E., Baker, P.J., Beckman, N.G., Coomes, D.A., Lines, E.R., Morris, W.K., Ruger, N., Alvarez, E., Blundo, C., Bunyavejchewin, S., Chuyong, G., Davies, S.J., Duque, A., Ewango, C.N., Flores, O., Franklin, J.F., Grau, H.R., Hao, Z., Harmon, M.E., Hubbell, S.P., Kenfack, D., Lin, Y., Makana, J.R., Malizia, A., Malizia, L.R., Pabst, R.J., Pongpattananurak, N., Su, S.H., Sun, I.F., Tan, S., Thomas, D., van Mantgem, P.J., Wang, X., Wiser, S.K., Zavala, M.A., 2014. Rate of tree carbon accumulation increases continuously with tree size. *Nature* 507, 90–93.
- Vermote, E.F., Tanré, D., Deuze, J.L., Herman, M., Morcette, J.-J., 1997. Second simulation of the satellite signal in the solar spectrum, 6S: an overview. *Geosci. Remote Sens., IEEE Trans.* 35, 675–686.
- Vose, J.M., Dougherty, P.M., Long, J.N., Smith, F.W., Gholz, H.L., Curran, P.J., 1994. Factors influencing the amount and distribution of leaf area of pine stands. *Ecol. Bull.*, 102–114.
- Wang, S., Zhou, L., Chen, J., Ju, W., Feng, X., Wu, W., 2011. Relationships between net primary productivity and stand age for several forest types and their influence on China's carbon balance. *J. Environ. Manage.* 92, 1651–1662.
- Wellburn, A.R., 1994. The spectral determination of chlorophylls a and b, as well as total carotenoids, using various solvents with spectrophotometers of different resolution. *J. Plant Physiol.* 144, 307–313.
- Wilson, E.H., Sader, S.A., 2002. Detection of forest harvest type using multiple dates of Landsat TM imagery. *Remote Sens. Environ.* 80, 385–396.
- Wu, C., Niu, Z., Tang, Q., Huang, W., 2008. Estimating chlorophyll content from hyperspectral vegetation indices: modeling and validation. *Agric. For. Meteorol.* 148, 1230–1241.
- Wu, C., Niu, Z., Tang, Q., Huang, W., Rivard, B., Feng, J., 2009. Remote estimation of gross primary production in wheat using chlorophyll-related vegetation indices. *Agric. For. Meteorol.* 149, 1015–1021.
- Wulder, M.A., White, J., Gillis, M., Walsworth, N., Hansen, M., Potapov, P., 2010. Multiscale satellite and spatial information and analysis framework in support of a large-area forest monitoring and inventory update. *Environ. Monit. Assess.* 170, 417–433.
- Zhang, Y., Chen, J.M., Thomas, S.C., 2007. Retrieving seasonal variation in chlorophyll content of overstory and understorey sugar maple leaves from leaf-level hyperspectral data. *Can. J. Remote Sens.* 33, 406–415.
- Zhang, Y., Chen, J.M., Miller, J.R., Noland, T.L., 2008. Leaf chlorophyll content retrieval from airborne hyperspectral remote sensing imagery. *Remote Sens. Environ.* 112, 3234–3247.
- Zhang, Q., Middleton, E.M., Margolis, H.A., Drolet, G.G., Barr, A.A., Black, T.A., 2009. Can a satellite-derived estimate of the fraction of PAR absorbed by chlorophyll (FAPAR<sub>chl</sub>) improve predictions of light-use efficiency and ecosystem photosynthesis for a Boreal aspen forest? *Remote Sens. Environ.* 113, 880–888.
- Zhu, Z., Foster, N.W., Arp, P.A., Meng, F., Bourque, C.P.A., 2004. A test and application of the model ForNBM in a northeastern Ontario jack pine (*Pinus banksiana* Lamb.) stand. *For. Ecol. Manage.* 193, 385–397.